Proceedings of the 21st ICSMGE, Vienna, Austria, 14 – 19 June 2026. Pistrol, Adam & Schweiger (eds.)
Published by: ÖGG, Austrian Society for Geomechanics, Salzburg, Austria, ISBN 978-3-9503898-4-5
https://doi.org/10.53243/ICSMGE2026-1513

Influence of Deep Foundations on High-Rise Buildings During a Seismic Impact

Cesar Alanoca
Postgraduate student, civil engineer, Saint Petersburg State University of Architecture and Civil Engineering (SPbGASU), Saint Petersburg, Russia, cesar_alanoca@outlook.com

Rashid Mangushev, Lidiia Kondratieva
Professor, Saint Petersburg State University of Architecture and Civil Engineering (SPbGASU), Saint Petersburg, Russia

ABSTRACT: The construction of earthquake-resistant high-rise buildings on weak soils requires careful consideration of the interaction within the "soil–foundation–high-rise building" system, which significantly affects the dynamic behavior during seismic events. The objective of this study was to perform a comparative analysis of the seismic response of a building with two types of foundations: (1) shallow foundations reinforced by jet grouting and (2) piled raft foundations. Numerical simulations were performed using the HS-small constitutive model in PLAXIS 3D, with comparisons to normative values according to Eurocode 8. The simulations revealed that piled raft foundations increased seismic accelerations at the upper floors by 23% (0.100g vs. 0.081g) and horizontal displacements by up to 5.0 cm compared to 0.9 cm for shallow foundations. The shear forces at the base for piled raft foundations were 5.7% higher (8206.2 kN/m vs. 7765.0 kN/m), but the PLAXIS 3D results were 27–31% lower than the Eurocode 8 standard values (11256.7 kN/m), demonstrating the conservative nature of the standard. The study confirms that piled raft foundations increase seismic demands despite their high bearing capacity, while shallow foundations with jet grouting better control deformations in weak soils. However, as this analysis was conducted under weak seismic conditions, caution is required in high-seismicity areas, where greater shear forces at the foundation base are expected, demanding optimized designs and additional seismic protection measures.

KEYWORDS: seismic resistance, high-rise buildings, weak soils, shallow foundation, piled raft foundation, jet grouting and PLAXIS 3D.

1 INTRODUCTION

The construction of high-rise buildings in earthquake-prone regions founded on weak soils demands special attention to foundation selection. Structural designers must consider not only the bearing capacity of the soil but also its dynamic behavior under seismic loading. This is particularly relevant since weak soils can significantly amplify seismic vibrations, increasing the potential for structural damage [1, 2].

The aim of this study is a comparative analysis of two types of foundations: (1) a shallow foundation reinforced by jet grouting and (2) a piled raft foundation. Both systems were modeled using PLAXIS 3D with the finite element method (FEM). The HS-small constitutive model was employed to capture the nonlinear behavior of the soil, particularly the variation of stiffness at small strains.

The results showed that the piled raft foundation, despite its superior bearing capacity, resulted in a 23% increase in seismic accelerations on the upper floors and horizontal displacements of up to 5.0 cm, compared to 0.9 cm for the shallow foundation. Moreover, standard calculations based on Eurocode 8 were excessively conservative for shallow foundations, overestimating the base shear forces by 27–31%.

Certain limitations of the study should be noted. The soil profile was simplified to two layers (loose and dense sand), and kinematic interaction between the piles and the superstructure was not fully considered. Furthermore, the analysis did not include the effects of soil liquefaction or variations in groundwater conditions.

2 MATERIAL AND METHOD

2.1 *Concept and Geometry*

The soil domain was modeled as a cube measuring 270 m × 270 m × 220 m, with the base embedded in bedrock. The upper layer consisted of 30 m of loose sand, underlain by 190 m of coarse sand. The superstructure modeled was a high-rise building with a height of 480 m and a square footprint of 77 m × 77 m (5929 m²). The underground portion comprised a two-story basement with a total depth of 10 m (5 m per floor).

The piled raft foundation employed bored piles with a diameter of 1.5 m and length of 80 m, anchored in the coarse sand layer.

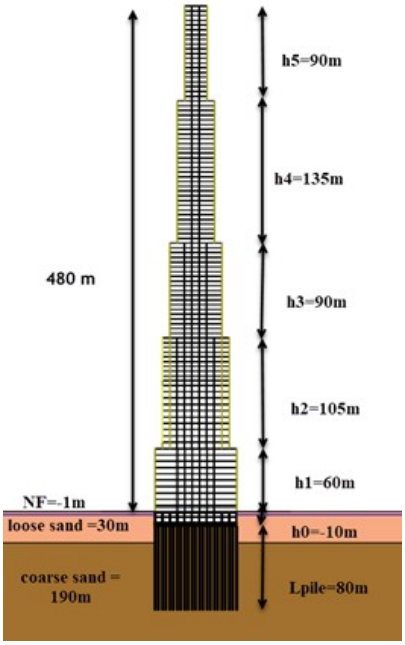

Figure 1. Conceptual model of the structure in AutoCAD.

2.2 *Material properties*

The main physical and mechanical characteristics of the soil layers, structural elements, and foundation components are presented in Tables 1 and 2. These data ensured the accuracy of the numerical simulations and the reliability of the verification process for the computational models.

Table 1. Soil Parameters for the HS-Small Model.

Parameter	Symbol	Top layer (Loose Sand)	Bottom layer (Coarse Sand)	Units.
Constitutive Model	-	HS small	HS small	-
Material Behaviour	Type	Undrained (A)	Undrained (A)	-
Unit Weight (above groundwater table)	γ_{unsat}	16	20	kN/m^3
Unit Weight (below groundwater table)	γ_{sat}	16	20	kN/m^3
Reference Stiffness in Triaxial Test	E_{50}^{ref}	10.5	60.0	Mpa
Reference Oedometer Stiffness	E_{oed}^{ref}	7.0	40.0	Mpa
Reference Unload/Reload Stiffness	E_{ur}^{ref}	35.0	200.0	Mpa
Stress Dependency	m	0.5	0.5	-
Effective Cohesion	c'_{ref}	0	0	kPa
Effective Internal Friction Angle	φ'	32	38	°
Dilatancy Angle	ψ	2	8	°
Shear Strain at Gs=0.722Go	$\gamma_{0.7}$	0.1078*10^{-3}	0.2190*10^{-3}	-
Small-Strain Shear Modulus	G_0^{ref}	75.54*10^3	123.2*10^3	kPa
Poisson's Ratio	υ'_{ur}	0.2	0.2	-
Reference Pressure	Pref	100	100	kPa
K_0 (At-Rest Earth Pressure Coefficient)	K_0	0.4701	0.3843	-

Table 2. Input Parameters for the Pile Elements.

Parameter	Symbol	Value	Units
Constitutive Model	—	Elastic	—
Young's Modulus	E	30×10^6	kN/m^2
Unit Weight	γ	25	kN/m^3
Pile Type	—	Predefined Solid Circular	—
Diameter	D	1.5	m
Cross-Sectional Area	A	1.767	m^2
Moment of Inertia	I	0.2485	m^4
Center-to-Center Pile Spacing (Out-of-Plane)	$L_{spacing}$	3.5	m
Axial Skin Resistance	T_{skin}	Layer - dependent	kN/m
Lateral Resistance	T_{max}	938,0	kN/m
Base Resistance	F_{max}	25,152.37	KN
Rayleigh Damping Coefficient (α)	α	0,2320	—
Rayleigh Damping Coefficient (β)	β	8.0×10^{-3}	—

2.3 *Dynamic analysis in PLAXIS 3D*

2.3.1 *Mesh Generation*

The minimum average shear wave velocity of the soil profile is Vs, min = 170 m/s, with a maximum input frequency of fmax = 2 Hz. The maximum allowable average element size for dynamic analysis was calculated as:

$$Average\ element\ size \leq \frac{V_{s,min}}{8*f_{max}} = \frac{170}{8*2} \approx 10.63\ m. \quad (1)$$

Table 3 summarizes the average element sizes used for different mesh densities.

Table 3. Average Element Sizes for Different Mesh Types.

Mesh Type	Scaling factor	Average Element Size (m)
Very Coarse	2	70.95
Coarse	1.5	53.22
Medium	1	35.48
Fine	0.7	24.83
Very Fine	0.5	17.74

2.3.2 *HS-Small Model in Seismic Analysis*

The Hardening Soil Small-Strain (HS-small) model extends the classical Hardening Soil (HS) model by incorporating the increased soil stiffness at small strains. This refinement is particularly important in seismic simulations, where accurate prediction of initial stiffness is essential.

The reference shear modulus for small strains, G0ref, defines the initial stiffness at infinitesimal strains. The degradation of shear stiffness with increasing strain γ is represented as:

$$\frac{G_s}{G_0} = \frac{1}{1+\left|\frac{\gamma}{\gamma_{0,7}}\right|} \quad (2)$$

Where G_s is the secant shear modulus at shear strain γ; G_0 is the initial shear modulus at the very small strains; γ is the shear strain; $\gamma_{0.7}$ is the shear strain at which the secant shear modulus G_s=0.722G_0, i.e., when the modulus has decreased to approximately 72,2% of its initial value.

Additionally, G_0 can be computed as:

$$G_0 = G_0^{ref}\left(\frac{c.cos\,\varphi - \sigma_3'\ sin\,\varphi}{c.cos\,\varphi + P_{ref}\ sin\,\varphi}\right)^m \quad (3)$$

where G_0^{ref} is the small-strain shear modulus; σ_3' is the effective minor principal stress; c – cohesion; φ is the internal friction angle; P_{ref} is the reference pressure, m is an exponent controlling stress-dependence.

This formulation allows the HS-small model to accurately reproduce nonlinear stress–strain behavior at small deformations, essential for dynamic and seismic analysis.

2.3.3 *Construction of FEM Models and Parameters*

The Hardening Soil Small-Strain (HS-small) model extends the classical Hardening Soil (HS) model by incorporating the increased soil stiffness at small strains. This refinement is particularly important in seismic simulations, where accurate prediction of initial stiffness is essential.

To analyze the seismic behavior of high-rise buildings on weak soils, two finite element models were developed: Model 1: High-rise building with shallow foundation, reinforced using jet grouting and Model 2: High-rise building with piled raft foundation.

Model 1 (Shallow Foundation): Soil reinforcement is implemented using jet grouting (injection of cement mortar). Grouting parameters: column diameter 1.2 m, spacing 2.5 m. The interaction between the cemented soil and the foundation slab is fully considered.

Model 2 (Piled Raft Foundation): Foundation consists of piles with a diameter of 1.5 m and a length of 80 m, embedded into a coarse sand layer. The grillage comprises a reinforced concrete slab 4 m thick. Full contact interaction between piles, soil, and slab is considered

2.3.4 *Modeling Stages*

Table 4 presents the sequence of calculations for Models 1 and 2. A staged construction procedure was used, including the sequential activation of structural components and application of loads, followed by dynamic analysis to accurately evaluate the foundation's response under seismic loading.

Table 4. Sequence of Calculation Stages.

Stage	Calculation Type	Description
Initial	K_0 Procedure	Generation of the initial stress state of the soil; structures deactivated.
Stage I	Static Analysis	Activation of structural elements; excavation to -10 m.
Stage II	Static Analysis	Application of horizontal loads; reset of displacements to zero.
Stage III	Dynamic Analysis	Dynamic analysis over a time interval of 5 seconds.
Stage IV	Dynamic Analysis	Re-analysis from initial conditions of Stage I; duration 10 seconds.

3 RESULTS AND DISCUSSION

3.1 *Seismic Response Analysis in PLAXIS 3D*

To evaluate the seismic response at both foundation and superstructure levels, control points were selected (Table 5).

Table 5. Coordinates of Control Points.

Point	Coordinates (x, y, z), m	Description
A	(38.5; 38.5; -220)	Bottom of the soil layer
B	(38.5; 38.5; -90)	Pile toe
C	(38.5; 38.5; -10)	Bottom of the foundation slab
D	(38.5; 38.5; -0.0)	First-floor slab
E	(38.5; 38.5; 255)	Top of the 50th floor
F	(38.5; 38.5; 480)	Top of the 100th floor

3.2 *Nonlinear Soil Behavior Analysis*

PLAXIS 3D employs the HS-small model, which captures the hysteretic behavior of soils during seismic events. The amplification factor of seismic vibrations within the soil was calculated using:

$$A.factor = \frac{a_{max}(D)}{a_{max}(A)} = \frac{0{,}027}{0{,}01} = 2{,}7 \quad (4)$$

This indicates an amplification of ground accelerations by 2.7 times in the upper layers due to the weak soil profile.

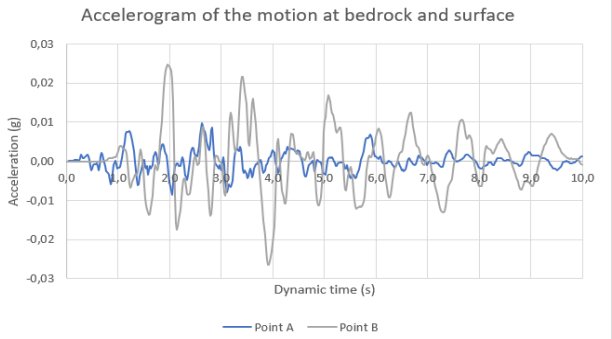

Figure 2. Free-field acceleration response.

3.3 *Analysis of shallow Foundations with Jet Grouting*

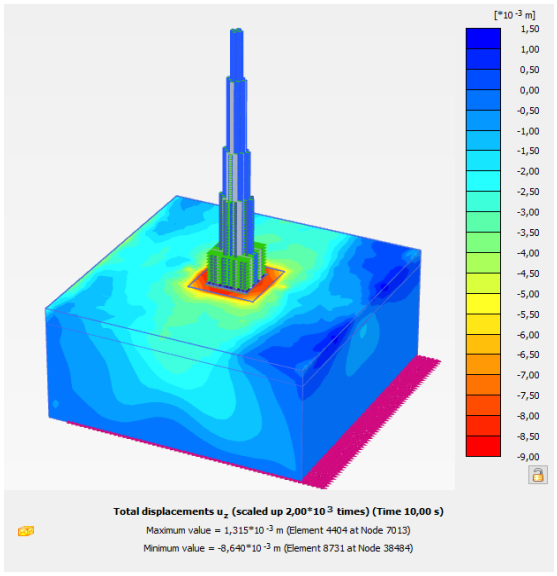

Figure 3. Vertical displacement, Uz = -0.864 cm under seismic loading.

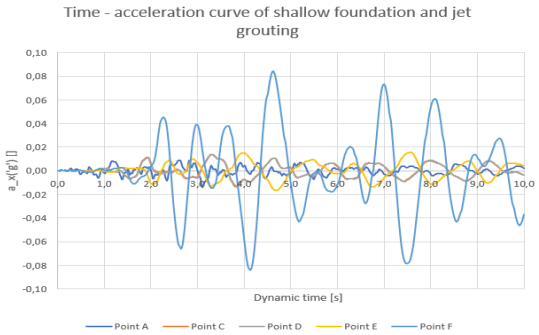

Figure 4. Acceleration time history for shallow foundation with jet grouting.

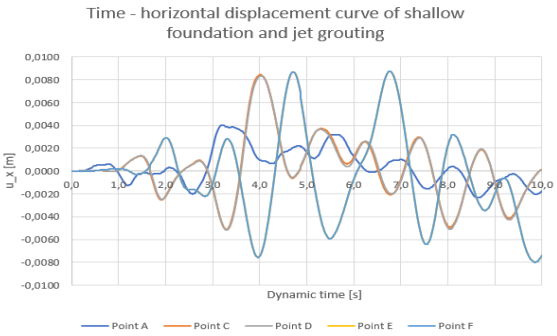

Figure 5. Horizontal displacement time history for shallow foundation with jet grouting.

Jet grouting effectively reduces deformations but does not fully compensate for the weakness of the soil. Maximum accelerations are recorded at the upper floors (ax = 0.081 g).

3.4 *Analysis of Piled Raft Foundation*

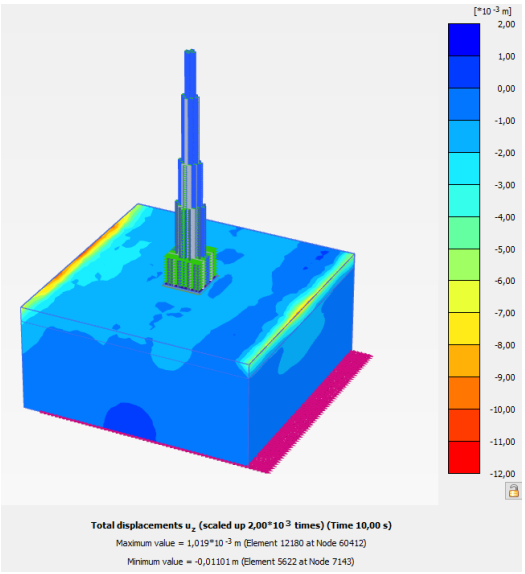

Figure 6. Vertical displacement, Uz = -1.101 cm under seismic loading.

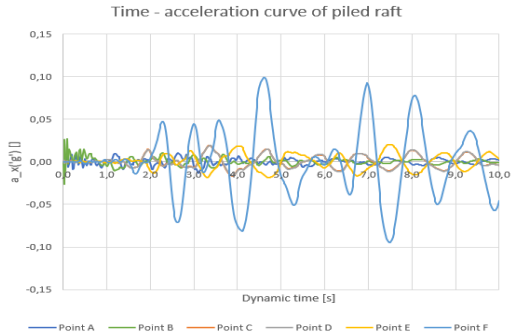

Figure 7. Acceleration time history for piled raft foundation.

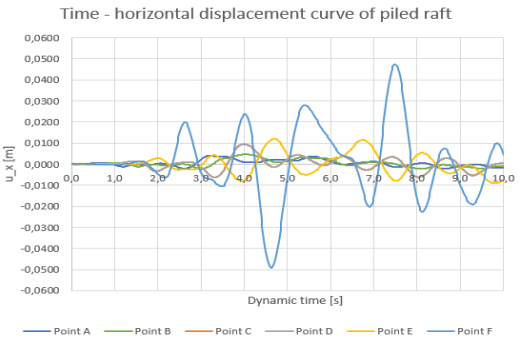

Figure 8. Horizontal displacement time history for piled raft foundation.

The piled raft foundation increases horizontal displacements up to 5.0 cm at the top of the structure (Point F). Shear forces at the foundation base are 5.7% higher than those of the shallow foundation system (Table 6).

Table 6. Shear Forces at the Foundation Base (kN/m).

Eurocode 8	PLAXIS 3D	
q= 1.0	Shallow Foundation + Jet Grouting	Piled Raft Foundation
11,256.7	7,765	8,206.2

Table 7. Comparison of Peak Accelerations and Displacements.

Point	Shallow Foundation		Piled Raft Foundation	
	a_x (g)	U_x (cm)	a_x (g)	U_x (cm)
C	0.018	0.85	0.025	1.25
F	0.081	0.90	0.100	5.00

4 CONCLUSIONS AND FUTURE WORK

This study analyzed the seismic response of high-rise buildings founded on weak soils using two foundation systems. The seismic input modeled corresponds to a weak earthquake (PGA = 0.01 g, ≈ M < 3.5 on the Richter scale), causing no significant damage. However, amplification of seismic accelerations to 0.027 g at the surface was observed due to the 30 m-thick weak soil layers. Weak soils significantly amplify seismic accelerations, necessitating enhanced structural strength and seismic design.

Piled raft foundations, while improving bearing capacity, transmit higher accelerations (+23%, 0.100 g vs. 0.081 g at Point F) and exhibit greater horizontal displacements (5.0 cm vs. 0.9 cm) compared to shallow foundations with jet grouting.

Shear force analysis indicates that Eurocode 8 tends to overestimate forces for shallow foundations, potentially leading to overly conservative designs. Conversely, the use of piles increased transverse forces by 5.7%, requiring detailed stability assessment.

Piled raft foundations enhance overall stability but also increase the transmission of seismic accelerations through the "soil–foundation–high-rise building" system. In regions of high seismicity (PGA = 0.4–0.8g), neglecting soil-structure interaction can result in substantial risks due to increased shear forces and horizontal displacements in the superstructure.

5 ACKNOWLEDGEMENTS

We thank the department of geotechnics at the University of St. Petersburg for their unconditional support in this research.

6 REFERENCES

Hamada, J. (2015). Bending moment of piles on piled raft foundation subjected to ground deformation during earthquake in centrifuge model test. Proceedings of the 15th Asian Regional Conference on Soil Mechanics and Geotechnical Engineering.

Hamada, M. (1991). Damage of piles by liquefaction-induced ground displacements. Proceedings of the Third US Conference on Lifeline Earthquake Engineering, Los Angeles, USA.

Hardin, B.O., & Drnevich, V.P. (1972). Shear modulus and damping in soils: Design equations and curves. Journal of the Soil Mechanics and Foundations Division (ASCE), 98(7), 667–692.

Martin, G.R., & Lam, I.P. (1995). Seismic design of pile foundations: Structural and geotechnical issues. Proceedings of the Third International Conference on Recent Advancements in Geotechnical Earthquake Engineering and Soil Dynamics, St. Louis, USA.

Mizuno, H. (1987). Pile damage during earthquakes in Japan (1923–1983). Proceedings of the ASCE Convention, Atlantic City, New Jersey, USA.